

# A Joint Experimental-Computational Comparative Study of the Pd(0)-Catalysed Reactions of Aryl Iodides and Aldehydes with N, O, and S Tethers

Daniel Solé,<sup>\*[a]</sup> Francesco Mariani,<sup>[a]</sup> and Israel Fernández<sup>\*[b]</sup>

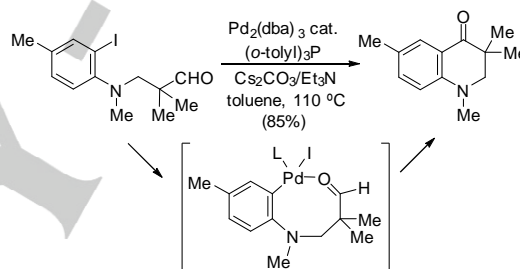
**Abstract:** The influence of the heteroatom (N, O and S) on the course of the palladium-catalysed intramolecular reactions of aryl iodides and aldehydes having heteroatom-containing tethers has been explored by an extensive experimental-computational (DFT) study. Two series of substrates have been considered, namely aldehydes bearing either the  $\alpha$ -(2-iodobenzylheteroatom) or  $\beta$ -(2-iodophenylheteroatom) moieties. While some experimental differences have been observed when changing from N to O or S in the 2-iodobenzyl series, the aldehydes in which the heteroatom is directly bonded to the aromatic ring showed a common chemical behaviour regardless of the heteroatom. The different reaction pathways leading to the experimentally observed reaction products have been studied by means of computational tools. Our calculations suggest that in all cases the initial nucleophilic addition involving a  $\sigma$ -aryl-Pd<sup>II</sup> intermediate is preferred over the competitive concerted metallation-deprotonation (CMD) process.

## Introduction

The ubiquity of heterocycles has prompted continuous efforts within the organic chemistry community to develop methodologies for their synthesis. In the last decade, the demand for more efficient heterocyclic syntheses has directed the research towards the development of catalytic processes based on the use of transition metals.<sup>[1]</sup> Besides its synthetic applications, transition metal chemistry involving heteroatom-containing compounds is of mechanistic interest due to its unique characteristics stemming from the heteroatom present in the substrates. Thus, in recent years, a number of examples have appeared highlighting the controlling or modifying role of heteroatoms in transition metal-promoted reactions.

As part of our ongoing program on the synthesis of nitrogen heterocycles,<sup>[2]</sup> we have been studying the palladium-catalysed intramolecular coupling of amino-tethered aryl iodides

and aldehydes. In this context, we recently described the palladium-catalysed intramolecular acylation<sup>[3]</sup> of (2-iodoanilino) aldehydes (Scheme 1), a reaction which is suggested to proceed through the nucleophilic addition of a readily formed  $\sigma$ -aryl-Pd<sup>II</sup> intermediate to the carbonyl group.<sup>[4,5]</sup> The preference for this reaction pathway over the possible C(=O)-H activation mechanism was ascribed to the high nucleophilicity of the carbon atom directly attached to the metal as a result of the  $\pi$ -donor effect of the *ortho*-nitrogen atom.<sup>[4a]</sup>



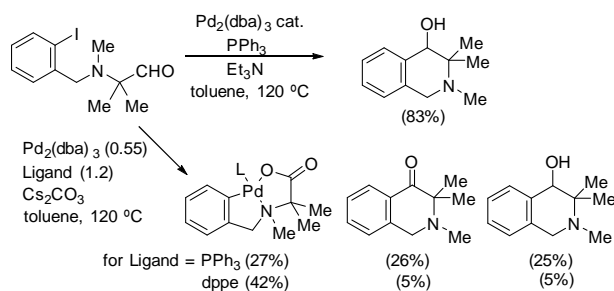
**Scheme 1.** Pd(0)-Catalysed intramolecular acylation of (2-iodoanilino) aldehydes.

We have also recently reported the palladium-catalysed reactions of  $\alpha$ -(2-iodobenzylamino) aldehydes, in which the nucleophilicity of the corresponding  $\sigma$ -aryl-Pd<sup>II</sup> intermediate is manifestly diminished. As a consequence, starting from these substrates, two competitive reaction pathways can be promoted by Pd(0), the selectivity of the process being controlled by the proper selection of the base (Scheme 2).<sup>[6]</sup> Thus, while the nucleophilic addition of the aryl-Pd<sup>II</sup> intermediate to the carbonyl group, giving a tetrahydroisoquinolin-4-ol derivative, is exclusively promoted by using Et<sub>3</sub>N, competition between a CO<sub>3</sub><sup>2-</sup>-mediated C-H bond-activation process and the nucleophilic addition occurs when using Cs<sub>2</sub>CO<sub>3</sub> as the base, thereby generating mixtures of addition products and tridentate [C,N,O] Pd(II) complexes. Our Density Functional Theory (DFT) calculations showed that in addition to the base, the coordination of the nitrogen atom to the metal centre along the reaction coordinate is also important for the control of the reaction pathway.<sup>[6]</sup>

The remarkable structure-dependent reactivity of these nitrogen-containing aldehydes is in sharp contrast to that observed in the carbocyclic series,<sup>[7]</sup> in which only the acylation reaction takes place.

[a] Prof. Dr. D. Solé, F. Mariani  
Laboratori de Química Orgànica, Facultat de Farmàcia  
Universitat de Barcelona  
Av. Joan XXIII s/n, 08028 Barcelona, (Spain)  
E-mail: [dsole@ub.edu](mailto:dsole@ub.edu)

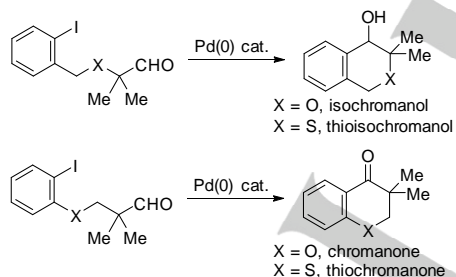
[b] Dr. I. Fernández  
Departamento de Química Orgánica I, Facultad de Ciencias  
Químicas, Centro de Innovación en Química Avanzada (ORFEO-  
CINQA)  
Universidad Complutense de Madrid  
Ciudad Universitaria, 28040 Madrid, (Spain)  
E-mail: [israel@quim.ucm.es](mailto:israel@quim.ucm.es)



**Scheme 2.** Pd(0)-Promoted reactions of  $\alpha$ -(2-iodobenzylamino) aldehydes.

Continuing our research in this chemistry, we were interested in exploring the influence of the heteroatom (changing from *N* to *O* or *S*) on the course of the palladium-catalysed reactions on these substrates. We hypothesised that the lesser extent of lone pair delocalisation when the heteroatom directly bonded to the aromatic ring is *O* or *S* could hinder the acylation reaction. Additionally, we wondered if the strong coordination ability of sulphur and the low oxophilicity of palladium could become an obstacle in the reactions of aldehydes bearing the 2-iodobenzyl-heteroatom moiety.

Herein, we report our studies on the palladium-catalysed intramolecular coupling reactions of aryl iodides and aldehydes in substrates with *O* or *S* tethers. The joint experimental-computational study on these reactions reveals both similarities and some differences with respect to their nitrogen-based counterparts and opens new synthetic entries to the chromane and isochromane nucleus, as well as their *S* analogues (Scheme 3).<sup>[8]</sup>



**Scheme 3.** Synthesis of *O* and *S* heterocycles.

## Results and Discussion

We commenced our investigation by focusing on the intramolecular coupling of sulfide **1** and ether **2**, the *S* and *O* analogues of  $\alpha$ -(2-iodobenzylamino) aldehydes, respectively. For the sake of comparison, a selection of the reaction conditions previously explored with the *N* containing series was used with aldehydes **1** and **2**. The results of these reactions are summarized in Table 1. Treatment of sulfide **1** with an equimolar amount of both Pd(0) and ligand in the presence of Cs<sub>2</sub>CO<sub>3</sub> resulted in the decomposition of the starting material (entry 1),

while the use of catalytic amounts of Pd(OAc)<sub>2</sub> and dppe,<sup>[9]</sup> maintaining Cs<sub>2</sub>CO<sub>3</sub> as the base, exclusively promoted the reduction of the aryl iodide of sulfide **1** to give **3** (entry 2 and Figure 1). In contrast, the latter reaction conditions with ether **2** led to the acylation ketone **5**, which was isolated in 30% yield (entry 5). All these results are very different from those obtained with  $\alpha$ -(2-iodobenzylamino) aldehydes, which in the presence of Cs<sub>2</sub>CO<sub>3</sub> led mainly to the formation of stable [C,*N*,*O*] Pd(II) complexes that divert the metal from the productive cycle, hindering the development of a catalytic cycle for the acylation reaction (Scheme 2).<sup>[6]</sup>

**Table 1.** Pd(0)-Catalysed coupling reactions of aldehydes **1** and **2**.<sup>[a]</sup>

Entry	Ald.	[Pd] [mol %] ligand [mol %]	Base [equiv.]	<i>t</i> [h]	Products (yield [%]) <sup>[b]</sup>
1	<b>1</b>	Pd <sub>2</sub> (dba) <sub>3</sub> (55) PPh <sub>3</sub> (120)	Cs <sub>2</sub> CO <sub>3</sub> (3)	24	---
2	<b>1</b>	Pd(OAc) <sub>2</sub> (20) dppe (25)	Cs <sub>2</sub> CO <sub>3</sub> (3)	72	<b>3</b> <sup>[c]</sup>
3	<b>1</b>	Pd(PPh <sub>3</sub> ) <sub>4</sub> (5)	Et <sub>3</sub> N (6)	72	<b>3</b> (25), <b>4</b> (64)
4	<b>1</b>	Pd <sub>2</sub> (dba) <sub>3</sub> (5) PPh <sub>3</sub> (11)	Et <sub>3</sub> N (6)	40	<b>3</b> : <b>4</b> (1:2) <sup>[d]</sup>
5	<b>2</b>	Pd(OAc) <sub>2</sub> (20) dppe (25)	Cs <sub>2</sub> CO <sub>3</sub> (3)	72	<b>5</b> (30) <sup>[e]</sup>
6	<b>2</b>	Pd(PPh <sub>3</sub> ) <sub>4</sub> (5)	Et <sub>3</sub> N (6)	72	<b>5</b> (31), <b>6</b> (42)
7	<b>2</b>	Pd <sub>2</sub> (dba) <sub>3</sub> (5) PPh <sub>3</sub> (11)	Et <sub>3</sub> N (6)	48	<b>6</b> (42) <sup>[f]</sup>
8	<b>2</b>	Pd(PPh <sub>3</sub> ) <sub>4</sub> (5)	Et <sub>3</sub> N (6) AcOK (1)	72	<b>5</b> (17), <b>6</b> (69)

[a] Reaction conditions: [Pd], ligand, and base (see table) in toluene at 120 °C in a sealed tube. [b] Isolated yields. [c] Yield not quantified. [d] <sup>1</sup>H NMR ratio, yield not quantified. [e] Trace amounts of the hydrodehalogenation product were also observed in the crude reaction mixture. [f] <sup>1</sup>H NMR ratio **5**:**6** (1:1.5).

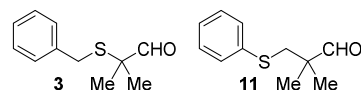


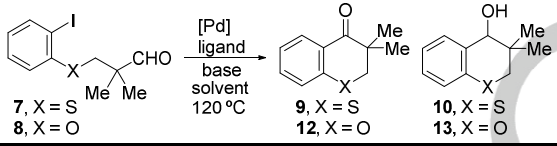
**Figure 1.** Reduction compounds **3** and **11**.

On the other hand, treatment of sulfide **1** with a catalytic amount of Pd(PPh<sub>3</sub>)<sub>4</sub> and Et<sub>3</sub>N as the base promoted the nucleophilic addition of the corresponding  $\sigma$ -aryl-Pd<sup>II</sup> intermediate to the carbonyl group to give alcohol **4** in 64% yield (entries 3). When submitted to the same reaction conditions,

ether **2** afforded a 1:1.4 mixture of ketone **5** and alcohol **6** (entry 6). Similar results were obtained when using Pd<sub>2</sub>(dba)<sub>3</sub>/PPh<sub>3</sub> as the catalyst (entries 4 and 7). Interestingly, when starting from

ether **2**, the addition of AcOK to otherwise the same reaction conditions resulted in an increase of the alcohol-to-ketone ratio, thus allowing **6** to be isolated in 69% yield (entry 8).

**Table 2.** Pd(0)-catalysed coupling reactions of aldehydes **7** and **8**.<sup>[a]</sup>



Entry	Ald.	Pd [mol %]/ligand [mol %]	Base [equiv.]	Solvent	t [h]	<sup>1</sup> H NMR ratio	Products (yield [%]) <sup>[b]</sup>
1	<b>7</b>	Pd <sub>2</sub> (dba) <sub>3</sub> (7.5)/( <i>o</i> -tolyl) <sub>3</sub> P (15)	Cs <sub>2</sub> CO <sub>3</sub> (3)/Et <sub>3</sub> N (6)	toluene	72	<b>9:11</b> (9:1)	<b>9</b> (43)
2	<b>7</b>	Pd <sub>2</sub> (dba) <sub>3</sub> (7)/( <sup>t</sup> Bu) <sub>3</sub> PH-BF <sub>4</sub> (14)	Cs <sub>2</sub> CO <sub>3</sub> (3)/Et <sub>3</sub> N (6)	toluene	72	<b>9:11</b> (2.6:1)	<b>9</b> (35)
3	<b>7</b>	Pd <sub>2</sub> (dba) <sub>3</sub> (7.5)/dtpf (15)	Cs <sub>2</sub> CO <sub>3</sub> (3)/Et <sub>3</sub> N (6)	toluene	72	<b>9:11</b> (8:1)	<b>9</b> (59)
4	<b>7</b>	Pd(PPh <sub>3</sub> ) <sub>4</sub> (10)	K <sub>3</sub> PO <sub>4</sub> (3)	toluene	72	<b>9:11</b> (3:1)	<b>9</b> (52), <b>11</b> (15)
5	<b>7</b>	Pd <sub>2</sub> (dba) <sub>3</sub> (7.5)/dtpf (15)	K <sub>3</sub> PO <sub>4</sub> (3)	THF	72	<b>9:11</b> (3.5:1)	<b>9</b> (36)
6	<b>7</b>	Pd(OAc) <sub>2</sub> (10)/dppe (25)	Cs <sub>2</sub> CO <sub>3</sub> (3)	toluene	72	---	--- <sup>[c]</sup>
7	<b>7</b>	Pd(OAc) <sub>2</sub> (10)/dtpf (11)	Cs <sub>2</sub> CO <sub>3</sub> (1)/Et <sub>3</sub> N (3)	DMF <sup>[d]</sup>	0.5	<b>9:10:11</b> (2:3:1)	<b>9</b> (20), <b>10</b> (30)
8	<b>7</b>	Pd(OAc) <sub>2</sub> (10)/dtpf (11)	AcOK (1)/Et <sub>3</sub> N (3)	DMF <sup>[d]</sup>	0.5	<b>9:10:11</b> (1:7:1.7)	<b>10</b> (42)
9	<b>7</b>	Pd(OAc) <sub>2</sub> (10)/( <i>o</i> -tolyl) <sub>3</sub> P (11)	AcOK (1)/Et <sub>3</sub> N (3)	DMF <sup>[d]</sup>	0.5	<b>9:10:11</b> (1:2.8:1)	--- <sup>[e]</sup>
10	<b>8</b>	Pd <sub>2</sub> (dba) <sub>3</sub> (7.5)/dtpf (15)	Cs <sub>2</sub> CO <sub>3</sub> (3)/Et <sub>3</sub> N (6)	toluene	45	---	<b>12</b> (89)
11	<b>8</b>	Pd(OAc) <sub>2</sub> (10)/dtpf (11)	AcOK (1)/Et <sub>3</sub> N (3)	DMF	48	---	<b>12</b> (20), <b>13</b> (55)
12	<b>8</b>	Pd <sub>2</sub> (dba) <sub>3</sub> (5)/PPh <sub>3</sub> (11)	AcOK (1)/Et <sub>3</sub> N (3)	DMF	60	<b>12:13</b> (1:2.6)	--- <sup>[e]</sup>
13	<b>8</b>	Pd <sub>2</sub> (dba) <sub>3</sub> (5)/PPh <sub>3</sub> (11)	AcOK (1)/Et <sub>3</sub> N (3)	toluene	72	<b>12:13</b> (1:3.8)	<b>13</b> (51)
14	<b>8</b>	Pd <sub>2</sub> (dba) <sub>3</sub> (5)/PPh <sub>3</sub> (11)	Et <sub>3</sub> N (3)	toluene	72	<b>12:13</b> (1:1.3)	--- <sup>[e]</sup>

[a] Reaction conditions: [Pd], ligand, base, and solvent (see table) at 120 °C in a sealed tube. [b] Isolated yields. [c] Decomposition. [d] The reaction was carried out in a sealed vessel in a microwave reactor (fixed temperature and variable pressure). [e] Yields not quantified.

Continuing with our comparative study, we then explored the palladium-catalysed reactions of aldehydes **7** and **8**, in which the heteroatom is directly bonded to the aromatic ring (Table 2). As commented above, the nitrogen-based counterparts of these compounds, the β-(2-iodoanilino) aldehydes, selectively undergo acylation through a mechanism involving carbopalladation between the aryl-Pd(II) intermediate and the carbonyl group. The preference for this process was ascribed to the high nucleophilicity of the carbon atom directly attached to the metal because of the π-donor effect of the *ortho*-nitrogen atom.<sup>[4a]</sup>

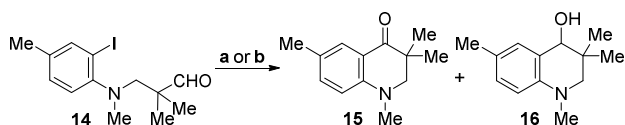
Under the reaction conditions developed for this intramolecular acylation (Scheme 1), involving the use of Cs<sub>2</sub>CO<sub>3</sub>/Et<sub>3</sub>N as the base in toluene,<sup>[4]</sup> sulfide **7** underwent the same reaction to give ketone **9**, although significant amounts of the hydrodehalogenation product **11** (Figure 1) were also invariably isolated (entries 1-3). The best results for the acylation of **7** were obtained when using dtpf as the ligand, which afforded

**9** in 59% yield (entry 3). Other combinations of ligand, base and solvent were also explored. The acylation reaction was still the main process when **7** was treated with Pd(PPh<sub>3</sub>)<sub>4</sub> as the catalyst and K<sub>3</sub>PO<sub>4</sub> as the base, allowing **9** to be isolated in 52% yield (entry 4). However, performing the reaction in THF (entry 5) or changing the ligand to dppe (entry 6) gave poor results. Interestingly, the use of the more polar solvent DMF together with a combination of Cs<sub>2</sub>CO<sub>3</sub> and Et<sub>3</sub>N as the base led to alcohol **10** as the main reaction product (entry 7). Changing the salt from Cs<sub>2</sub>CO<sub>3</sub> to AcOK increased the formation of **10**, which was isolated in 42% yield when dtpf was used as the ligand (entry 8).

When ether **8** was submitted to the conditions optimised for the reaction with sulfide **7**, acylation was the only reaction pathway observed, which allowed the preparation of ketone **12** in 89% yield (entry 10). Also, starting from ether **8** and performing the reaction in DMF in the presence of AcOK

reproduced the behaviour previously observed with sulfide **7**. Under these conditions **8** afforded alcohol **13** as the main reaction product (entry 11). Changing the ligand to  $\text{PPh}_3$  resulted in a 1:2.6 alcohol-to-ketone ratio (entry 12). Finally, alcohol **13** was still obtained as the main product when the reactions of **8** were performed using  $\text{Et}_3\text{N}$  as the base in toluene, either with or without AcOK (entries 13-14).

In this context, it should be noted that the palladium-catalysed reaction of 2-iodoaniline **14** either in DMF in the presence of AcOK or using  $\text{Et}_3\text{N}$  as the base in toluene led also to mixtures of ketone **15** and alcohol **16** (Scheme 4). Leaving aside minor differences, these results confirm that sulfide **7**, ether **8** and aniline **14** show the same behaviour in their palladium-catalysed reactions.



**Scheme 4.** Reagents and conditions: (a)  $\text{Pd}_2(\text{dba})_3$  (0.05),  $\text{PPh}_3$  (0.1),  $\text{Et}_3\text{N}$  (6), toluene, 120 °C, 52 h, 17% (**15**), 32% (**16**); (b)  $\text{Pd}(\text{OAc})_2$  (0.1), dtpf (0.11), KOAc (1),  $\text{Et}_3\text{N}$  (3), DMF, 120 °C, 52 h, 45% (**15**), 20% (**16**).

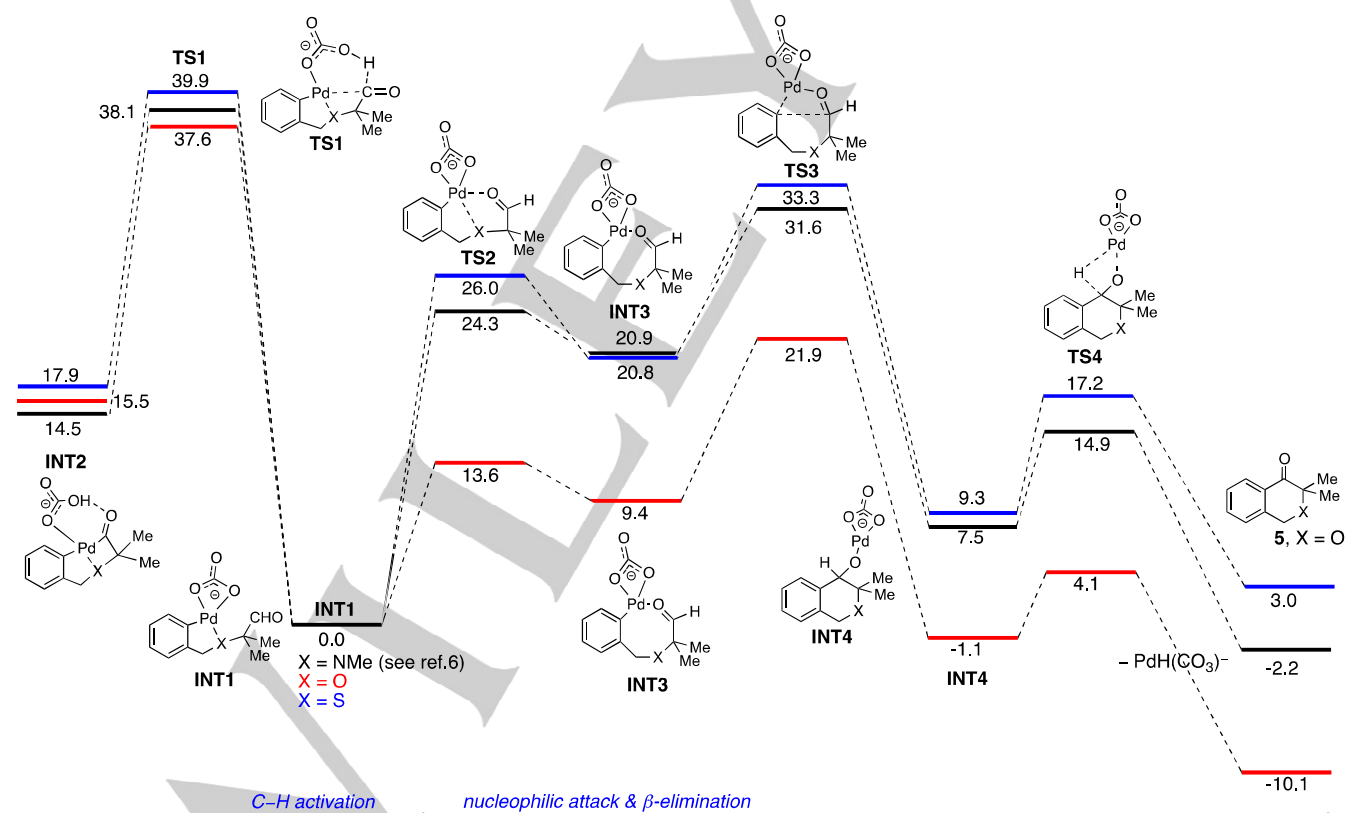


**Figure 2.** Computed reaction profiles starting from  $\text{INT1-X}$  ( $\text{X} = \text{NMe}, \text{O}, \text{and S}$ ). Relative free energy values ( $\Delta G_{393}$ , computed at 120 °C) are given in kcal mol<sup>-1</sup>. All data have been computed at the PCM(toluene)-B3LYP/def2-TZVP/B3LYP/def2-SVP level.

Our calculations indicate that the reaction profiles involving the different heteroatoms ( $X = \text{N}, \text{O}, \text{S}$ ) are quite similar. Of course, differences in the computed relative free energies are found as a consequence of their distinct donor/coordination abilities. Despite that, it becomes clear that in all cases the concerted metalation-deprotonation (CMD) process, mediated by carbonate and leading to the C–H activation product **INT2**, is associated with a quite high activation barrier ( $\Delta G^\ddagger = 39.9, 38.1$  and  $37.6$  kcal/mol, for  $X = \text{S}, \text{NMe}$  and  $\text{O}$ , respectively). At variance, the nucleophilic addition reaction which begins with the initial  $X$  to C=O ligand exchange via **TS2** proceeds comparatively with a much lower energetic cost. As a consequence, starting from ether **2**, the formation of ketone **5** via **INT2** by a reductive elimination reaction<sup>[6]</sup> seems clearly unfeasible. Moreover, the formation of the corresponding tridentate [C,X,O]-Pd<sup>II</sup> complex from **INT2** is not expected for  $X = \text{O}$ , and only products derived from the nucleophilic addition should be experimentally found. This computational prediction is in nice agreement with the experimental findings, as ketone **5** was isolated in the process involving ether **2** when  $\text{Cs}_2\text{CO}_3$  was used as the base (see entry 5, Table 1). This reaction product derives therefore from a nucleophilic addition reaction (which affords the alkoxide-palladium intermediate **INT4** via **TS3**, with an activation barrier of 12.5 kcal/mol) and subsequent  $\beta$ -elimination reaction via **TS4** ( $\Delta G^\ddagger = 5.2$  kcal/mol).

Our calculations also indicate that the reactions involving sulfide **1** show a reaction profile much more similar to its nitrogen counterpart. However, only the reduction product **3** was experimentally isolated (see entry 2, Table 1). This suggests that the reduction process<sup>[11]</sup> from intermediates **INT1** or **INT3** or even from the initially formed aryl-palladium intermediate having

a Pd-iodide bond is faster than the nucleophilic addition reaction. This is compatible with the high computed free energy difference between the corresponding transition state **TS3** and the initial complex **INT1** ( $\Delta G = 33.3$  kcal/mol, see Figure 2).

In addition, we have also computed the reaction profiles depicted in Figure 2 at the PCM(toluene)-B3LYP-D3/def2-TZVP//B3LYP/def2-SVP level to account for dispersion effects. From the data in Figure S1 (see supporting information), it becomes evident that the inclusion of dispersion in the calculations does not modify the above described scenario, i.e. the nucleophilic addition/ $\beta$ -elimination pathway is preferred over the demanding C–H activation pathway (activation barriers ca. 38 kcal/mol).

On the other hand, in the presence of  $\text{Et}_3\text{N}$  as base instead of  $\text{Cs}_2\text{CO}_3$  sulfide **1** affords alcohol **4** (entries 3-4, Table 1), whereas ether **2** leads to a mixture of the corresponding alcohol **6** and ketone **5** (entries 6-7, Table 1). Thus, the behaviour of the sulfide resembles, once again, that found for its nitrogen counterpart, which exclusively produces the corresponding isoquinolin-4-ol derivative when the reaction is conducted in the presence of  $\text{Et}_3\text{N}$ .<sup>[6]</sup> This was ascribed to the coordination of the nitrogen atom to the palladium which hinders the *cisoid* conformation required for the  $\beta$ -elimination step leading to the corresponding isoquinolone.<sup>[6]</sup> Our calculations indicate that a similar coordination from the sulphur atom in the related **INT6-S** also occurs after the corresponding nucleophilic addition step (Figure 3a). Therefore, alcohol **4** should be exclusively formed from **INT6-S** via a well-known  $\text{Et}_3\text{N}$ -mediated reductive protonation process,<sup>[2a,12]</sup> as experimentally observed.

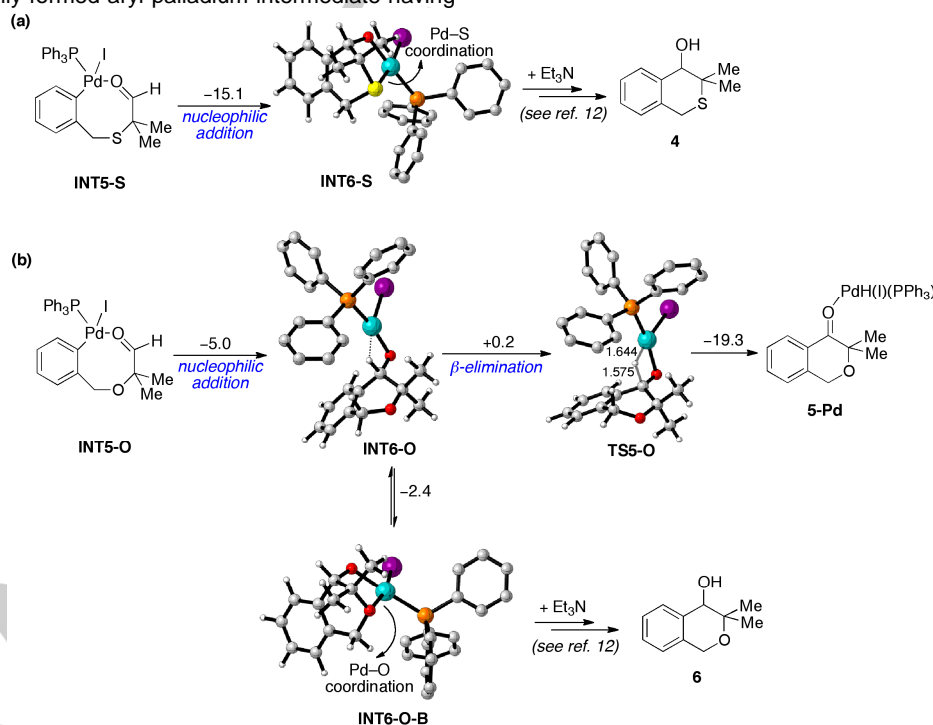


**Figure 3.** Computed reaction profiles starting from **INT5-S** (a) and **INT5-O** (b). Relative free energy values ( $\Delta G_{393}$ , computed at 120 °C) and bond distances are given in kcal mol<sup>-1</sup> and angstroms, respectively. All data have been computed at the PCM(toluene)-B3LYP/def2-TZVP//B3LYP/def2-SVP level.



In contrast, the nucleophilic addition step from the oxygen derivate **INT5-O** leads to the formation of **INT6-O**, which possesses the *cisoid* conformation required for the  $\beta$ -elimination step forming ketone **5** (via **TS5-O**, computed activation barrier of only 0.2 kcal/mol, see Figure 3b). Interestingly, **INT6-O** is in equilibrium with the **INT6-O-B**, an intermediate which resembles **INT6-S**, therefore having a Pd-O coordination and evolving to the alcohol **6**. The coexistence of both intermediates (free energy difference of only 2.4 kcal/mol) is responsible for the observed mixture of reaction products and finds its origin in the low coordination ability of the oxygen atom as compared to nitrogen or sulphur. Indeed, this is reflected in the much lower computed Pd-X Wiberg Bond Order in **INT6-O-B** as compared to **INT6-S** (0.12 vs 0.43 au, for X = O and S, respectively) and in the lower exergonicity computed for the **INT5-X**→**INT6-X** transformation (-7.4 and -15.1 kcal/mol for X = O and S, respectively).

DFT calculations were carried out as well to explore the effect of the heteroatom in this series of compounds where the

heteroatom is directly attached to the *ortho*-position of the aryl group. Again, the reaction profiles depicted in Figure 4 shows the possible competitive reaction pathways for the conversion of **INT7** (the species formed upon initial oxidative addition of **7**, **8** and the analogous aniline derivate) into the experimentally observed ketones **9**, **12** and **9N**, respectively.

Our calculations indicate that the formation of the respective ketone does not come from the carbonate mediated (CMD) process leading to the C-H activation product **INT9**. This is again due to the quite high activation barrier computed for this transformation, which involves the transition states **TS6** ( $\Delta G^\ddagger = 38.8, 35.4$  and  $31.9$  kcal/mol, for X = O, S and NMe, respectively). Therefore, chromanone **9**, thiochromanone **12** and dihydroquinolinone **9N** result again from a nucleophilic addition reaction followed by a  $\beta$ -elimination step, which proceed with a comparatively much lower energetic cost.

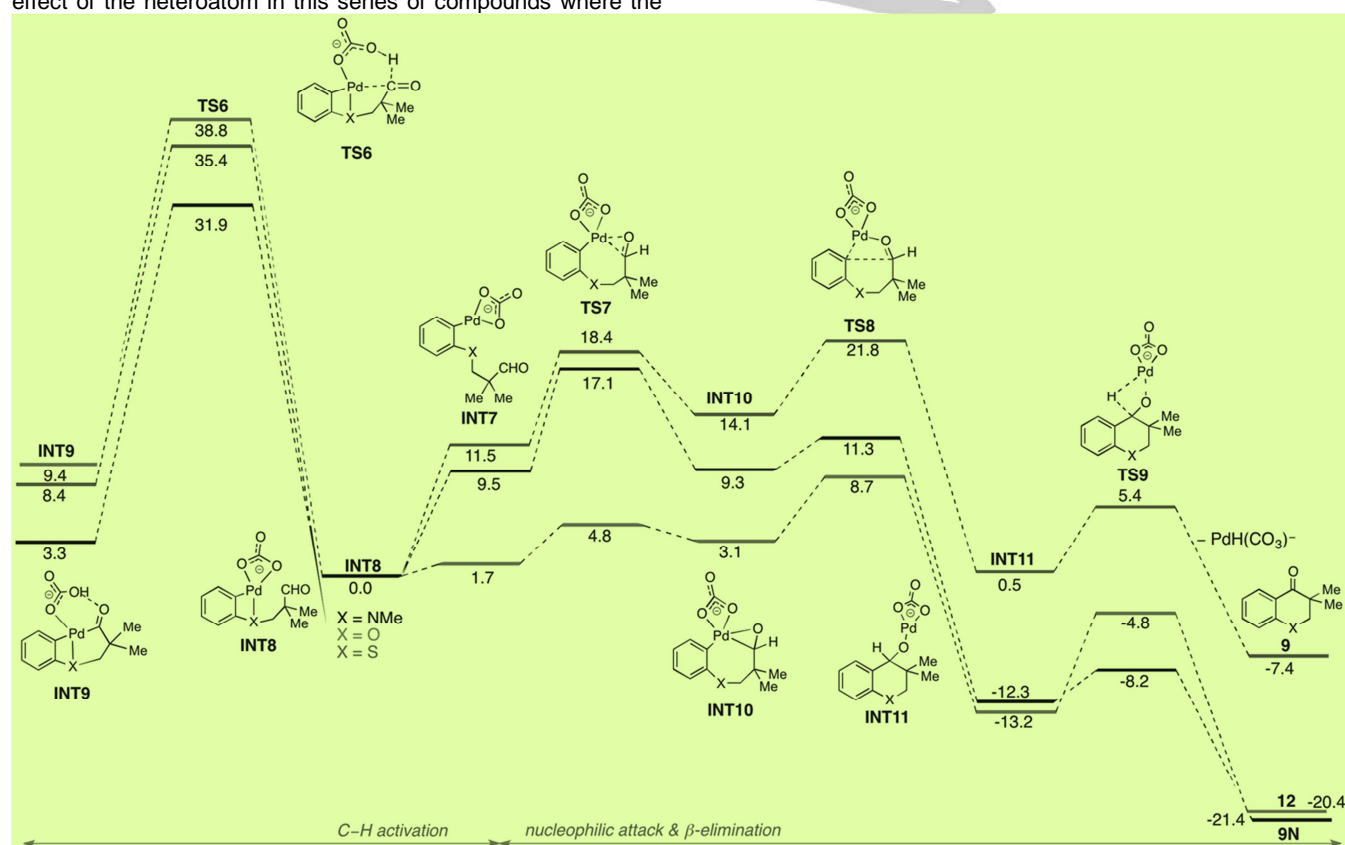


**Figure 4.** Computed reaction profiles starting from **INT7-X** (X = NMe, O, and S). Relative free energy values ( $\Delta G_{393}$ , computed at 120 °C) are given in kcal mol<sup>-1</sup>. All data have been computed at the PCM(toluene)-B3LYP/def2-TZVP/B3LYP/def2-SVP level.

Interestingly, the influence of the heteroatom is significant in the initial intramolecular nucleophilic addition reaction, as confirmed by the different computed activation barriers involving **TS8** ( $\Delta G^\ddagger = 2.0, 5.6$  and  $7.7$  kcal/mol, for X = NMe, O and S, respectively). This can be ascribed to the extent of the delocalization of the corresponding heteroatom lone-pair (LP)

into the aryl moiety, which controls the relative nucleophilicity of the carbon atom directly attached to the transition metal in **INT10**. Indeed, according to the second-order perturbation theory (SOPT) of the NBO method, the SOPT-energy associated with such delocalization in **INT10-X** varies  $\Delta E^{(2)} = -$

33.2 > -21.5 > -14.6 kcal/mol, for X = NMe, O, S, respectively, thus paralleling the computed trend in activation barriers.

The influence of the heteroatom is further reflected in the HOMO-LUMO interaction. As shown in Figure 5, the HOMO of **INT10-N** can be viewed as a  $\pi$ -molecular orbital which involves both the LP of the nitrogen atom and the carbon atom attached to palladium. The LUMO can be considered as the  $\pi^*(\text{C}=\text{O})$  involving the coordinated carbonyl group.

Similar molecular orbitals have been computed for **INT10-O** (and **INT10-S**) with the exception that in these species the HOMO of **INT10-N** corresponds to the HOMO-1. Despite that, the HOMO-LUMO gap in the nitrogen derivative is significantly reduced (3.90 eV) as compared to the HOMO-1-LUMO gap computed for its oxygen counterpart (4.26 eV). As a result of a more favorable HOMO-LUMO interaction, a lower reaction barrier should be expected for **INT10-N**, which agrees with the values computed for the nucleophilic addition reaction.

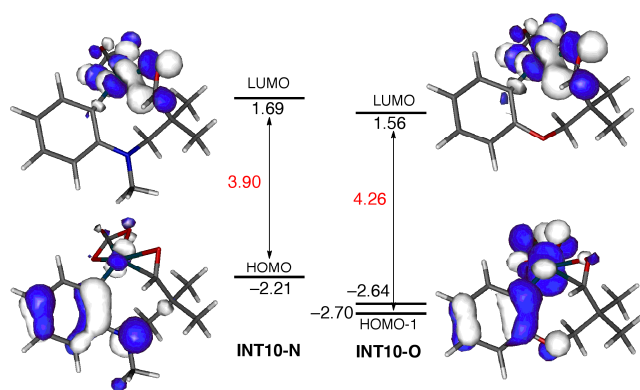


**Figure 5.** Computed molecular orbitals involved in the intramolecular nucleophilic addition reaction of **INT10**. Orbitals energies are given in eV. All data have been computed at the B3LYP/def2-SVP level.

Interestingly, both the sulfide **7** and the ether **8** afford the corresponding alcohols, **10** and **13** respectively, in addition to the ketones **9** and **12** when the reaction is conducted in DMF as solvent (entries 7-9 and 11-12, Table 2). Our calculations indicate that the activation barrier of the  $\beta$ -elimination step leading to ketones **9** and **12** increases in the solvent DMF (9.2 kcal/mol for **INT11-S**, and 8.9 kcal/mol for **INT11-O**) compared to toluene (4.9 kcal/mol for **INT11-S**, and 8.4 kcal/mol for **INT11-O**). Additionally, the highly solvating/coordinating ability of the DMF (as compared to toluene) would lead to a more facile transmetalation of the Pd<sup>II</sup> alkoxide **INT11** to give the corresponding cesium or potassium alkoxide, which after protonolysis during the workup would give the alcohol.<sup>[2a]</sup> As a consequence of both effects, significant amounts of the corresponding alcohols are experimentally observed (see Table 2).

## Conclusions

The joint experimental-computational comparative study reported herein has clarified the influence of the heteroatom (changing from *N*, to *O* and *S*) on the course of the palladium-catalyzed intramolecular reactions of aryl iodides and aldehydes tethered by heteroatom-containing chains. Two alternative reaction pathways can be envisaged to explain the formation of the observed ketone derivatives when the reaction is conducted in the presence of Cs<sub>2</sub>CO<sub>3</sub>, namely C–H activation versus nucleophilic attack followed by  $\beta$ -elimination. Although some differences in the computed relative free energies have been found as a consequence of either the distinct coordination ability of the heteroatom or the delocalization of the heteroatom lone-pair into the aryl fragment, our calculations indicate that, in all cases, the nucleophilic addition reaction followed by  $\beta$ -elimination proceeds with a much lower energetic cost than the concerted metalation-deprotonation (CMD) process. Therefore, it can be concluded that the nature of the heteroatom in the initial aryl iodide is not decisive in the outcome of the reaction.

## Experimental Section

### General

All commercially available reagents were used without further purification. <sup>1</sup>H- and <sup>13</sup>C NMR spectra were recorded using Me<sub>4</sub>Si as the internal standard, with a Varian Gemini 300 or a Varian Mercury 400 instrument. Chemical shifts are reported in ppm downfield ( $\delta$ ) from Me<sub>4</sub>Si for <sup>1</sup>H and <sup>13</sup>C NMR. TLC was carried out on SiO<sub>2</sub> (silica gel 60 F<sub>254</sub>, Merck), and the spots were located with UV light or 1% aqueous KMnO<sub>4</sub>. Flash chromatography was carried out on SiO<sub>2</sub> (silica gel 60, SDS, 230-400 mesh ASTM). Unless otherwise noted, all experiments were performed in an argon atmosphere. Drying of organic extracts during workup of reactions was performed over anhydrous Na<sub>2</sub>SO<sub>4</sub>.

### Typical method for the Pd(0)-catalysed reactions

A mixture of aldehyde **1** (70 mg, 0.22 mmol), Et<sub>3</sub>N (0.18 mL, 1.32 mmol), Pd(PPh<sub>3</sub>)<sub>4</sub> (13 mg, 0.011 mmol) in toluene (7 mL) was stirred at 120 °C in a sealed tube for 72 h. The reaction mixture was partitioned between saturated NaHCO<sub>3</sub> aqueous solution and Et<sub>2</sub>O. The organic extracts were washed with brine, dried, and concentrated. The residue was purified by chromatography (from hexanes to hexanes-EtOAc 4:1) to give **3** (10 mg, 25%) and **4** (27 mg, 64%).

## Computational Details

All the calculations reported in this paper were obtained with the GAUSSIAN 09 suite of programs.<sup>[13]</sup> Electron correlation was partially taken into account using the hybrid functional usually denoted as B3LYP<sup>[14]</sup> using the double- $\zeta$  quality plus polarization def2-SVP basis set<sup>[15]</sup> for all atoms. Reactants and products were characterized by frequency calculations,<sup>[16]</sup> and have positive definite Hessian matrices. Transition structures (TS's) show only one negative eigenvalue in their diagonalized force constant matrices, and their associated eigenvectors were confirmed to correspond to the motion along the reaction coordinate under consideration using the Intrinsic Reaction Coordinate (IRC) method.<sup>[17]</sup> Solvents effects were taken into account using the Polarizable Continuum Model (PCM).<sup>[18]</sup> Single point calculations (PCM-B3LYP/def2-

TZVP) on the gas-phase optimized geometries were performed to estimate the change in the Gibbs energies (at 393.15 K) in the presence of toluene or DMF as solvent using the triple- $\zeta$  quality plus polarization def2-TZVP basis set.<sup>[15]</sup> This level is denoted PCM-B3LYP/def2-TZVP//B3LYP/def2-SVP. For the reaction profiles depicted in Figure 2, dispersion effects were taken into account using the D3-correction described by Grimme and co-workers.<sup>[19]</sup>

Wiberg Bond Indices (WBIs) and donor-acceptor interactions have been computed using the natural bond orbital (NBO) method.<sup>[20]</sup> The energies associated with these two-electron interactions have been computed according to the following equation:

$$\Delta E_{\phi\phi^*}^{(2)} = -n_{\phi} \frac{\langle \phi^* | \hat{F} | \phi \rangle^2}{\epsilon_{\phi^*} - \epsilon_{\phi}}$$

where  $\phi$  and  $\phi^*$  are two filled and unfilled Natural Bond Orbitals having  $\epsilon_{\phi}$  and  $\epsilon_{\phi^*}$  energies, respectively;  $n_{\phi}$  stands for the occupation number of the filled orbital.

## Acknowledgements

We gratefully acknowledge financial support for this work from the Spanish MINECO-FEDER (CTQ2012-31391, CTQ2013-44303-P and Red de Excelencia Consolider CTQ2014-51912-REDC).

**Keywords:** catalysis • cyclization • heterocycles • Density Functional Theory calculations • palladium

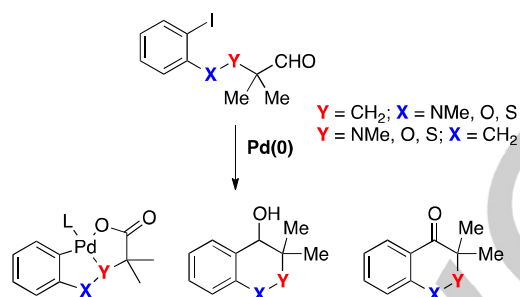
- [1] Recent reviews: a) J. J. Li, G. W. Gribble, *Palladium in Heterocyclic Chemistry: A Guide for the Synthetic Chemist*, Pergamon, Amsterdam, **2000**; b) E. Negishi, Ed. *Handbook of Organopalladium Chemistry for Organic Synthesis*; Wiley-VCH: New York, **2002**, Vols. I and II; c) J., Tsuji, Ed. *Palladium in Organic Synthesis, in Topics in Organometallic Chemistry*; Springer-Verlag: Berlin, **2005**; d) G. Zeni, R. C. Larock, *Chem. Rev.* **2006**, *106*, 4644; e) I. V. Seregin, V. Gevorgyan, *Chem. Soc. Rev.*, **2007**, *36*, 1173; f) F. Bellina, R. Rossi, *Tetrahedron* **2009**, *65*, 10269; g) M. Platon, R. Amardeil, L. Djakovitch, J.-C. Hierso, *Chem. Soc. Rev.*, **2012**, *41*, 3929; h) B. Alcaide, P. Almendros, C. Aragoncillos, *Chem. Soc. Rev.* **2014**, *43*, 3106; i) see also, E. Soriano, I. Fernández, *Chem. Soc. Rev.* **2014**, *43*, 3041, and references therein.
- [2] a) D. Solé, L. Vallverdú, X. Solans, M. Font-Bardia, J. Bonjoch, *J. Am. Chem. Soc.* **2003**, *125*, 1587; b) D. Solé, X. Urbaneja, J. Bonjoch, *Tetrahedron Lett.* **2004**, *45*, 3131; c) D. Solé, O. Serrano, *J. Org. Chem.* **2008**, *73*, 2476; d) D. Solé, O. Serrano, *J. Org. Chem.* **2010**, *75*, 6267; e) D. Solé, M.-L. Bannasar, I. Jiménez, *Org. Biomol. Chem.*, **2011**, *9*, 4535; f) D. Solé, I. Fernández, M. A. Sierra, *Chem. Eur. J.* **2012**, *18*, 6950; g) D. Solé, I. Fernández, *Acc. Chem. Res.* **2014**, *47*, 168.
- [3] For the Pd(0)-catalysed intermolecular acylation of aryl bromides with aldehydes, see: P. Nareddy, C. Mazet, *Chem. Asian J.* **2013**, *8*, 2579.
- [4] a) D. Solé, F. Mariani, I. Fernández, M. A. Sierra, *J. Org. Chem.* **2012**, *77*, 10272; b) D. Solé, F. Mariani, *J. Org. Chem.* **2013**, *78*, 8136. See also reference [2g].
- [5] For the Pd(0)-catalysed intramolecular acylation with esters and amides, see: a) D. Solé, O. Serrano, *Angew. Chem. Int. Ed.* **2007**, *46*, 7270; b) D. Solé, O. Serrano, *J. Org. Chem.* **2008**, *73*, 9372.
- [6] D. Solé, F. Mariani, I. Fernández, *Adv. Synth. Catal.* **2014**, *356*, 3237.
- [7] a) P. Álvarez-Bercedo, A. Flores-Gaspar, A. Correa, R. Martín, *J. Am. Chem. Soc.* **2010**, *132*, 466; b) A. Flores-Gaspar, A. Gutiérrez-Bonet, R. Martín, *Org. Lett.* **2012**, *14*, 5234.
- [8] For recent examples on the metal catalysed synthesis of these heterocyclic systems, see: a) P. W. Davies, S. J.-C. Albrecht, *Angew. Chem. Int. Ed.* **2009**, *48*, 8372; b) J. Zhang, L. Wei, *Chem. Commun.*, **2012**, 2636; c) Q. Liu, K. Wen, Z. Zhang, Z. Wu, Y. J. Zhang, W. Zhang, *Tetrahedron* **2012**, *68*, 5209; d) K. R. Prasad, C. Nagaraju, *Org. Lett.* **2013**, *15*, 2778; e) E. Coutant, P. C. Young, G. Barker, A.-L. Lee, *Beilstein J. Org. Chem.* **2013**, *9*, 1797; f) T.-S. Zhu, J.-P. Chen, M.-H. Xu, *Chem. Eur. J.* **2013**, *19*, 865; g) S. E. Ammann, G. T. Rice, M. C. White, *J. Am. Chem. Soc.* **2014**, *136*, 10834; h) H. Murase, K. Senda, M. Senoo, T. Hata, H. Urabe, *Chem. Eur. J.* **2014**, *20*, 317.
- [9] It is well known that Pd(OAc)<sub>2</sub> is reduced to Pd(0) in the presence of phosphines, see for example: C. Amatore, L. El Kaïm, L. Grimaud, A. Jutand, A. Meignié, G. Romanov, *Eur. J. Org. Chem.* **2014**, 4709.
- [10] See Computational Details.
- [11] The formation of hydrodehalogenation compounds has been reported in many different Pd(0)-catalyzed reactions starting from aryl halides. The exact mechanism of this reduction, as well as the identity of the reducing agent could be diverse. See for example: a) K. H. Shaughnessy, B. C. Hamann, J. F. Hartwig, *J. Org. Chem.* **1998**, *63*, 6546; b) L. G. Quan, M. Lamrani, Y. Yamamoto, *J. Am. Chem. Soc.* **2000**, *122*, 4827; c) K. Högenauer, J. Mulzer, *Org. Lett.* **2001**, *3*, 1495; d) A. A. Pletnev, R. C. Larock, *J. Org. Chem.* **2002**, *67*, 9428.
- [12] C. C. Lu, J. C. Peters, *J. Am. Chem. Soc.* **2004**, *126*, 15818.
- [13] Gaussian 09, Revision D.01, M. J. Frisch, G. W. Trucks, H. B. Schlegel, G. E. Scuseria, M. A. Robb, J. R. Cheeseman, G. Scalmani, V. Barone, B. Mennucci, G. A. Petersson, H. Nakatsuji, M. Caricato, X. Li, H. P. Hratchian, A. F. Izmaylov, J. Bloino, G. Zheng, J. L. Sonnenberg, M. Hada, M. Ehara, K. Toyota, R. Fukuda, J. Hasegawa, M. Ishida, T. Nakajima, Y. Honda, O. Kitao, H. Nakai, T. Vreven, J. A. Montgomery, Jr., J. E. Peralta, F. Ogliaro, M. Bearpark, J. J. Heyd, E. Brothers, K. N. Kudin, V. N. Staroverov, R. Kobayashi, J. Normand, K. Raghavachari, A. Rendell, J. C. Burant, S. S. Iyengar, J. Tomasi, M. Cossi, N. Rega, J. M. Millam, M. Klene, J. E. Knox, J. B. Cross, V. Bakken, C. Adamo, J. Jaramillo, R. Gomperts, R. E. Stratmann, O. Yazyev, A. J. Austin, R. Cammi, C. Pomelli, J. W. Ochterski, R. L. Martin, K. Morokuma, V. G. Zakrzewski, G. A. Voth, P. Salvador, J. J. Dannenberg, S. Dapprich, A. D. Daniels, Ö. Farkas, J. B. Foresman, J. V. Ortiz, J. Cioslowski, and D. J. Fox, Gaussian, Inc., Wallingford CT, 2009
- [14] a) A. D. Becke, *J. Chem. Phys.* **1993**, *98*, 5648; b) C. Lee, W. Yang, R. G. Parr, *Phys. Rev. B* **1998**, *37*, 785; c) S. H. Vosko, L. Wilk, M. Nusair, *Can. J. Phys.* **1980**, *58*, 1200.
- [15] F. Weigend, R. Alhrichs, *Phys. Chem. Chem. Phys.* **2005**, *7*, 3297.
- [16] J. W. McIver, A. K. Komornicki, *J. Am. Chem. Soc.* **1972**, *94*, 2625.
- [17] C. González, H. B. Schlegel, *J. Phys. Chem.* **1990**, *94*, 5523.
- [18] a) S. Miertuš, E. Scrocco, J. Tomasi, *Chem. Phys.* **1981**, *55*, 117; b) J. L. Pascual-Ahuir, E. Silla, I. Tuñón, *J. Comp. Chem.* **1994**, *15*, 1127; c) V. Barone, M. Cossi, *J. Phys. Chem. A*, **1998**, *102*, 1995.
- [19] S. Grimme, J. Antony, S. Ehrlich, H. Krieg, *J. Chem. Phys.* **2010**, *132*, 154104.
- [20] a) J. P. Foster, F. Weinhold, *J. Am. Chem. Soc.* **1980**, *102*, 7211; b) A. E. Reed, F. Weinhold, *J. Chem. Phys.* **1985**, *83*, 1736; c) A. E. Reed, R. B. Weinstock, F. Weinhold, *J. Chem. Phys.* **1985**, *83*, 735; d) A. E. Reed, L. A. Curtiss, F. Weinhold, *Chem. Rev.* **1988**, *88*, 899.



## Entry for the Table of Contents

## FULL PAPER

**Heteroatom Effect:** The influence of the heteroatom on the outcome of intramolecular palladium-catalysed reactions of aryl iodides and aldehydes is explored by means of experimental and computational tools.



Daniel Solé,<sup>[a]</sup> Francesco Mariani,<sup>[a]</sup> and Israel Fernández<sup>[b]</sup>

Page No. – Page No.

**A Joint Experimental-Computational Comparative Study of the Pd(0)-Catalysed Reactions of Aryl Iodides and Aldehydes with N, O, and S Tethers**